processes

MDPI

Article

Comparative Analysis of the Interaction between the Antiviral Drug Umifenovir and Umifenovir Encapsulated in Phospholipids Micelles (Nanosome/Umifenovir) with dsDNA as a Model for Pharmacogenomic Analysis by Electrochemical Methods

Victoria V. Shumyantseva [1,2,*], Tatiana V. Bulko [1], Lyubov E. Agafonova [1], Veronika V. Pronina [1] and Lyubov V. Kostryukova [1]

[1] Institute of Biomedical Chemistry, Pogodinskaya Street 10, Moscow 119121, Russia; tanyabulko@mail.ru (T.V.B.); agafonovaluba@mail.ru (L.E.A.); veronicapunch@mail.ru (V.V.P.); kostryukova87@gmail.com (L.V.K.)

[2] Department of Biochemistry, Pirogov Russian National Research Medical University, Ostrovitianov Street 1, Moscow 117997, Russia

* Correspondence: viktoria.shumyantseva@ibmc.msk.ru; Tel.: +7-4-992-465-820

Abstract: In the present study, the electrochemical behavior of antiviral drug umifenovir (Umi) and umifenovir encapsulated in phospholipids micelles (nanosome/umifenovir, NUmi) were investigated for the first time on screen-printed electrodes modified by carbon nanotubes. We have shown that Umi can be electro oxidized around the potential of +0.4 V in the concentration range of 50–500 μM (R^2 = 0.992). Non-overlapping signatures of DNA and umifenovir (10–150 μM) permit to register interaction between umifenovir (or umifenovir encapsulated in phospholipids micelles), purine, and pyrimidine heterocyclic bases of DNA separately. The type of interaction is most likely via electrostatic interactions and groove binding in drug-DNA formed complex, as was revealed based on the values of binding constants Kb and the cathodic shifts of oxidation potentials for heterocyclic bases with increasing Umi or NUmi concentration. The negative values of Gibbs free energy (Δ*G*) for all nucleobases confirm the process spontaneity. This study is the first one presenting the effect of antiviral drug umifenovir and umifenovir encapsulated in phospholipids micelles on dsDNA as a target of pharmacogenomics.

Keywords: DNA; umifenovir; phospholipids micelles; drug-DNA interaction; electrochemistry; electrochemical biosensor; differential pulse voltammetry

Citation: Shumyantseva, V.V.; Bulko, T.V.; Agafonova, L.E.; Pronina, V.V.; Kostryukova, L.V. Comparative Analysis of the Interaction between the Antiviral Drug Umifenovir and Umifenovir Encapsulated in Phospholipids Micelles (Nanosome/Umifenovir) with dsDNA as a Model for Pharmacogenomic Analysis by Electrochemical Methods. *Processes* **2023**, *11*, 922. https://doi.org/10.3390/pr11030922

Academic Editor: Alina Pyka-Pająk

Received: 17 February 2023
Revised: 10 March 2023
Accepted: 15 March 2023
Published: 17 March 2023

1. Introduction

Umifenovir (Arbidol, ethyl 6-bromo-4-[(dimethylamino)methyl]-5-hydroxy-1-methyl-2-[(phenylsulfanyl)methyl]-1H-indole-3-carboxylate, Scheme 1) is the broad spectrum drug for the prevention and treatment of viral infections [1].

Umifenovir (Umi) is effective against both enveloped and nonenveloped DNA and RNA viruses, and are used for treating influenza. Umifenovir specifically inhibits in vitro Influenza virus type A, B, pathogenic subtypes A (H1N1)pdm09, and A(H5N1), as well as other viruses that cause ARVI (acute respiratory viral infections): coronavirus associated with severe acute respiratory syndrome (SARS), adenovirus (Adenovirus), rhinovirus (Rinovirus), respiratory syncytial virus (Pneumovirus), and parainfluenza virus (Paramyxovirus). Umifenovir is effective against human herpes virus, hepatitis B and C virus, Ebola virus, inhibits enterovirus C, and possess antioxidant activity [2–8].

Umi belongs to fusion inhibitors, interacts with the hemagglutinin of the viruses, and prevents the fusion of the lipid envelope of the virus and cell membranes. It has interferon-inducing activity in a study on mice, the induction of interferons was noted already after

16 h, and high titers of interferons remained in the blood up to 48 h after administration. Umi stimulates cellular and humoral immune reactions, such as increasing the number of lymphocytes in the blood, especially T-cells (CD3), increases the number of T-helpers (CD4) without affecting the level of T-suppressors (CD8), normalizes the immunoregulatory index, stimulates the phagocytic function of macrophages, and increases the number of natural killer (NK-cells). Umi inhibits the activity of SARS-CoV (COVID-19), the target of this interaction is large Spike proteins on the virus surface (S-protein of the cell membrane of the virus), and also interacts with the hemagglutinin of the virus and prevents the fusion of the lipid envelope of the virus and cell membranes [1–3]. Umi having one dimethyl amino group and nitrogen groups contacted tightly with ACE-2 from COVID-19 via electrostatic interaction with acidic amino acids at the ACE-2 contact site [9]. It is possible to predict that Umi molecules can also interact through electrostatic mode with negatively charged groups of biomolecules, such as nucleic acids.

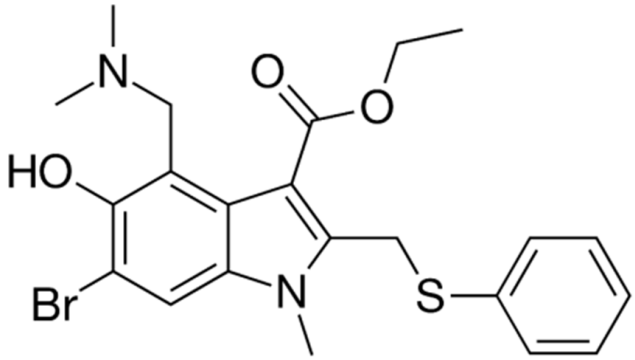

Scheme 1. Molecular structure of Umifenovir (Arbidol).

Therapeutic efficacy in viral infections is manifested in a decrease in the duration and severity of the course of the disease and its main symptoms, as well as a decrease in the incidence of complications associated with a viral infection and exacerbations of chronic bacterial diseases. The therapeutic dose of umifenovir is 800 mg/day for 5 days [8].

As has been shown, incorporation of drug into nanoparticles or nanocarriers to treat and diagnose diseases has tremendous advantages and perspectives [10]. The development of drug-delivery systems to organs, tissues, and cells as targets eliminates many shortcomings of the drugs under development and existing drugs, such as low water solubility, rapid sorption or metabolism in the body, the difficulty of penetrating cell membranes, and the blood-brain barrier. The use of drug-delivery systems possesses a broad spectrum of advantages. Incorporation of drugs into nanoparticles makes it possible to prolong the action of the medicinal compound and to improve biocompatibility. Appropriated drug-delivery system protects the medicinal preparation from premature biodegradation and increases the bioavailability of the drug, overcoming biological barriers. Different types of nanoplatforms permit to carry out tissue-directed and/or target-specific transport of the drug compound; provide controlled release of the drug compound; maintain the optimal therapeutic concentration of the drug compound in the blood and tissues; minimize the side effects of the drug compound and its metabolites. This is especially important for drugs, the use of which in free forms is limited by their pronounced toxicity. Various materials (gold nanoparticles, dendrimers, polymers, etc.) are used in the development of drug transport systems [11,12]. One of the ways to increase the bioavailability, therapeutic efficacy of drugs, reduce their toxicity, and reduce side effects is to supply them with transport systems based on phospholipids nanoparticle, since such systems are biodegradable, do not cause allergic reactions, and the surface of nanoparticles can be modified for the insertion or bringing of additional targeted properties [10–13]. A change in the pharmacokinetics of drugs when they are included in phospholipid nanoparticles leads to the fact that a significant reduction in the dose of the drug is possible to achieve a therapeutic effect [13].

Umi embedded into phospholipid nanoparticles (nanosome/umifenovir, NUmi) from soy phosphatidylcholine with the addition of sodium oleate was prepared according to technology that was elaborated earlier [13,14].

Despite the development of approaches for construction of drug-delivery systems based on plant phospholipids and the proven therapeutic efficacy of therapeutic agents in the composition of phospholipid nanoparticles, the direction associated with the peculiarities of the interaction of such forms of drugs with molecular targets, such as DNA, remains unexplored. The development of more efficient, cost-effective methods for modelling the metabolism of drugs in biosystems is one of the fastest growing areas of bioanalytical chemistry. Modelling of metabolic pathways for the transformation of new drugs, physiologically active compounds is carried out both "in silico", and experimentally "in vivo", "in vitro" and "in electrode" using enzyme systems [15].

DNA is a main participant in genomics and proteomics. DNA plays a key role in transcription, translation, replication, and division processes. From another side, genome DNA, mitochondrial DNA, virus DNA, and short non-complementary DNA may be pharmacological targets of a huge number of drug formulations [16–18]. The binding processes of drug molecules to or onto DNA can dramatically change the properties of DNA leading to disruption in the whole genome, and in turn, in transcriptome functioning.

To study the mechanisms of DNA/drug interaction, chromatographic, UV-Vis-spectral methods (absorption spectroscopy), nuclear magnetic resonance (NMR), FTIR spectroscopic measurements, electrophoretic methods, luminescent and fluorescent methods, atomic force microscopy (AFM), isothermal titration calorimetry, and mass spectrometry are widely used [19,20].

Electrochemical methods for DNA analysis and drug-DNA interaction possess high sensitivity and registration of concentration dependent "response" of heterocyclic nucleobases on drug influence [16,17,19–28]. The investigation of peculiarities and the mode of medications' interaction with DNA is an important part of rational drug design construction of new and more efficient therapeutic agents and prediction of drug influence on genomic processing. Examining the electrochemical signals of DNA or DNA/drug complex before and after interaction argues interaction and helps in drug-target mechanism elucidation. In electrochemical studies, using DNA sensor constructions, intercalative interaction mode is described by a shift in oxidation peak towards positive potential as thermodynamically unfavorable process, while electrostatic interaction involves peak shift towards negative oxidation potential [26–28]. The use of disposable screen-printed planar electrodes with a minimum diameter of the working electrode (1–2 mm) makes it possible to miniaturize and standardize the analytical procedures.

The aim of this study was to find out the effects of Umi and NUmi as drug with broad spectrum of pharmacological activity onto the dsDNA molecule via the registration of electrochemical oxidation signals of guanine, adenine, and thymine. This study is the first investigation of antiviral drug Umi and NUmi with dsDNA as a pharmacological target from pharmacogenomics viewpoint.

2. Materials and Methods

2.1. Reagents

Umi drug substance was obtained from "CHEM" LTD (Kuzmalovsky settlement, Leningrad Region, Russia). Umifenovir composition incorporated in phospholipid-oleate nanoparticles (phospholipid-based umifenovir drug delivery system, nanosomal umifenovir, NUmi), was prepared in accordance with [13,14].

Stock solution of Umi was prepared as 2.5 mM (1.2 mg/mL) in hot distilled water with ultrasonic disintegration during 3 min. NUmi solutions in distilled water were prepared with the same concentration as Umi.

Water dispersion of 0.4% single-wall carbon nanotubes (SWCNT, diameter 1.6 ± 0.4 nm, length >5 μM, surface area 1000 m^2/g) TUBALL™ BATT H_2O stabilized by carboxymethylcellulose was obtained from OCSIAL Ltd. (https://ocsial.com, Oksial Additives NSK

LLC, Novosibirsk, Russia). Potassium phosphate monobasic (≥99%) and potassium phosphate dibasic trihydrate (≥99%) were purchased from Sigma-Aldrich (St. Louis, MO, USA). Sodium chloride (99.5%) was purchased from Acros Organics Organics (Janssen Pharmaceuticalaan 3a, B-2440, Geel, Turnhout 73.440, Belgium).

Fish-sperm double-stranded DNA (dsDNA, from herring sperm as lyophilized powder) was obtained from Sigma-Aldrich (D 3159). All other chemicals were of analytical grade and used without further purification. All aqueous solutions were prepared using Milli-Q water (18.2 MΩcm) purified with a Milli-Q water purification system by Millipore (Frankfurter Strasse 250, 64293 Darmstadt, Germany).

The stock solution of DNA (1.5 mg/mL) was prepared in 100 mM potassium phosphate buffer with 50 mM NaCl (pH 7.4), as described previously [19,21]. The purity of the DNA stock solution was checked by taking the absorbance ratio of A_{260}/A_{280}, which was found to be in the range of 1.8–1.9 indicating there is no contamination of protein in ds-DNA solution [29].

2.2. Electrochemical Equipment

Screen-printed electrodes (SPE) with graphite working (geometric area 0.0314 cm^2), auxiliary electrodes, and silver/silver chloride reference electrode (Ag/AgCl) were obtained from ColorElectronics, Russia (http://www.colorel.ru, accessed on 1 September 2022).

Electrochemical measurements were performed using a potentiostat/galvanostat PG-STAT 12 Autolab (Metrohm Autolab, The Netherlands, accessed on 1 February 2020). operated by the GPES software (version 4.9.7). All electrochemical measurements were carried out at room temperature as +23 °C in 0.1 M potassium phosphate buffer with 50 mM NaCl as supporting electrolyte (PBS, pH 7.4). The DPV technique was employed in order to follow direct electrochemical oxidation of dsDNA. The following DPV parameters were used: potential range of 0.2–1.2 V, pulse amplitude of 0.025 V, potential step of 0.005 V, pulse duration of 50 ms, modulation amplitude of 0.05 V. All potentials were referred to the Ag/AgCl reference electrode. Triplicated measurements have been performed for electrochemical estimation of varying concentrations of DNA. These values were within 10–12% (the relative standard deviation, RSD = 10–12%) that highlights the inherent repeatability of the electrochemical setup.

2.3. Preparation of Electrochemical Sensors

The working electrodes were modified by 2 μL of preliminarily 5 times diluted in distilled water dispersion of SWCNT TUBALL™ BATT H_2O. Electrodes SPE/SWCNT stayed at room temperature until complete drying.

For further incorporation of the dsDNA, 60 μL of the dsDNA solution (1.5 mg/mL) prepared in PBS, pH 7.4 was dropped onto the surface of modified electrode and incubated for 15 min before measurements. Horizontal regimen of measurement was used for all experiments. For the investigation of DNA-drug interaction, a complex of DNA with Umi was formed at specified concentrations of pharmaceutical formulations, and constant concentration of DNA as 1.5 mg/mL and was incubated 15 min before adsorption onto electrode surface [21,25,27]. DPV measurements were performed after 60 s deposition time.

3. Results and Discussion

3.1. Electrochemical Behavior of Umi on SPE/SWCNT

An indole derivative umifenovir (Arbidol, ethyl 6-bromo-4-[(dimethylamino)methyl]-5-hydroxy-1-methyl-2-[(phenylsulfanyl)methyl]-1H-indole-3-carboxylate) is widely used drug for the prevention and treatment of COVID-19 and some other viral infections [2,9,30]. We have studied electrochemical behavior of Umi on the screen-printed electrodes modified with single-wall carbon nanotubes. Disposable screen-printed electrodes were used due to their commercial availability, relatively low cost, wide opportunities and range of modification methods, and adaptability for on-site measurements. Carbon nanomaterials significantly improve the sensitivity of electrodes [31].

Cyclic voltammograms (CV) for the 500 µM Umi in the potential range of 0 V to 1.1 V were investigated in electrolyte buffer corresponding to physiological media (PBS, pH 7.4). Umi exhibited a single irreversible anodic peak at E = +0.4 V (Figure 1A) of unsubstituted aromatic ring hydroxylation. A broad shoulder is appeared at higher scan rates and may be attributed to the possible sulfur oxidation [32,33].

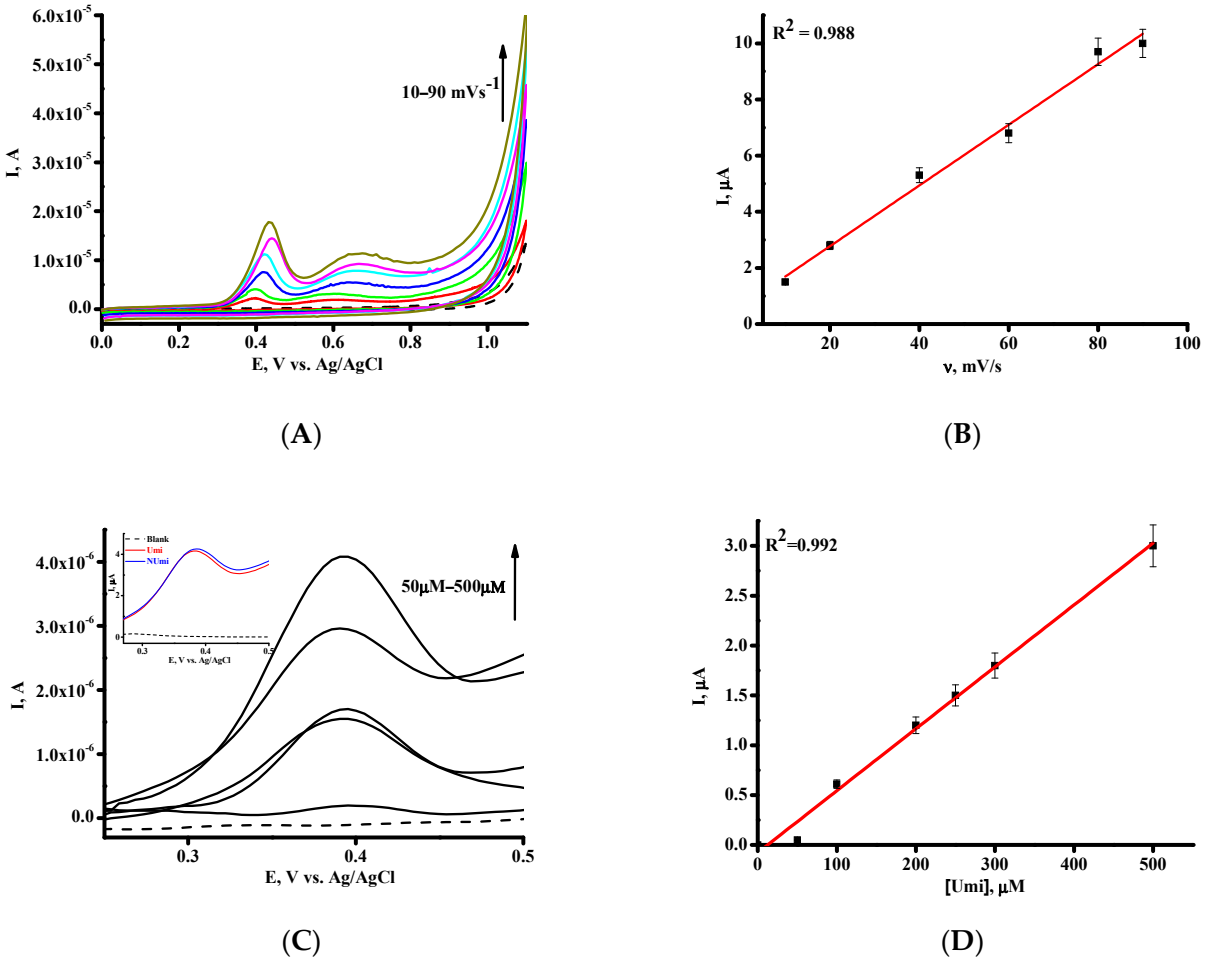

Figure 1. (**A**) CV of 500 µM Umi on SPE/SWCNT at different scan rates from 10 to 90 mV/s; (**B**) The plot of the oxidation peak current vs. the scan rate; (**C**) DP voltammograms recorded in PBS (pH 7.4) with increasing Umi concentration in the range of 50–500 µM. Dashed black line represents DPV of SPE/SWCNT in supporting electrolyte. The relative standard deviation of the DPV response on the SPE/SWCNT for three experiments was ±5%; Inset: DPV of 500 µM Umi and NUmi; (**D**) DPV peak current versus the concentration of Umi.

Irreversible oxidation of Umi at E = +0.4 V with linear dependence of peak current versus the scan rate confirms surface character of electrochemical process (Figure 1A,B) [34–36]. The dependence between the Umi concentration and corresponding differential pulse voltammetry (DPV) peak current at 0.388 ± 0.002 V demonstrated linear character in the concentration range of 50–500 µM (R^2 = 0.992, Figure 1C,D). NUmi demonstrated the same position of oxidation peak with comparable intensity of electrooxidation (Inset of Figure 1C). Table 1 represents the characteristics of calibration curve. The limit of detection (LOD) and the limit of quantification LOQ) were calculated from the calibration curve as kSD/b (k = 3 for LOD, k = 10 for LOQ), b = slope of the calibration curve, SD = standard deviation of the intercept [26,37] (Table 1).

Table 1. Electroanalytical parameters of quantitative Umi assay with SPE/SWCNT.

Parameters	DPV
E_{ox}, V	0.388 ± 0.002
Sensitivity, μA/μM (Slope)	0.53
Linear range, μM	50–500
Limit of quantification LOQ, μM	50
Limit of detection LOD, μM	17
Equation for linear regression *	Iox = 0.0062 ± 0.0002 [Umi] − 0.076 ± 0.059
Correlation coefficient, R^2	0.992

* Iox corresponds to the oxidative currents (peak heights) for Umi; [Umi] is a concentration of Umi in μM that was deposited onto the working surface area of SPE/SWCNT.

Based on DPV of Umi and using Equation (1), it is calculated that one electron is involved in the oxidation process of this drug (Figure 1C) [34–36].

$$W_{1/2} = 3.52\, RT/nF, \quad (1)$$

where $W_{1/2}$ is the DPV half peak width, R is gas constant, 8.3145 J $K^{-1}mol^{-1}$, T is temperature, in Kelvin, F is Faraday constant 96,485 C mol^{-1}.

We used drug concentrations range of 10–150 μM for the investigation of the interaction of native dsDNA with Umi or NUmi.

3.2. Electrochemical Behavior of DNA on SPE/SWCNT

DNA electrochemical oxidation was studied on SPE/SWCNT after deposition of DNA on the surface of the modified electrodes. The method of physical entrapment of the DNA molecules onto SWCNT support in the electrode was used for DNA immobilization.

Figure 2A depicts the cyclic voltammograms (CVs) of dsDNA (1.5 mg/mL) on SPE/SWCNT in the range of potentials of 0 V to 1.2 V at scan rates from 10 to 300 mV/s. Only oxidation peaks were observed for guanine and adenine, confirming the irreversible electrochemical processes. At the scan rates in the range of 10 to 300 mV/s, the oxidation peak currents increase linearly (Figure 2B,C). These dependences suggest the surface-controlled process [34–36].

The DPV was used for the determination of concentration dependences of DNA peak currents. The concentration-dependent appearance of the oxidation peaks of the DNA nucleobases, such as purine bases guanine (G), adenine (A) at ~0.6 V, at ~0.9 V and pyrimidine base thymine (T) at ~1.1 V, were registered, respectively (Figure 3A).

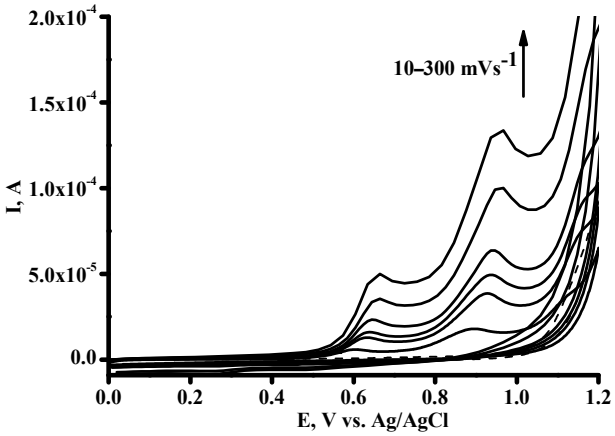

(**A**)

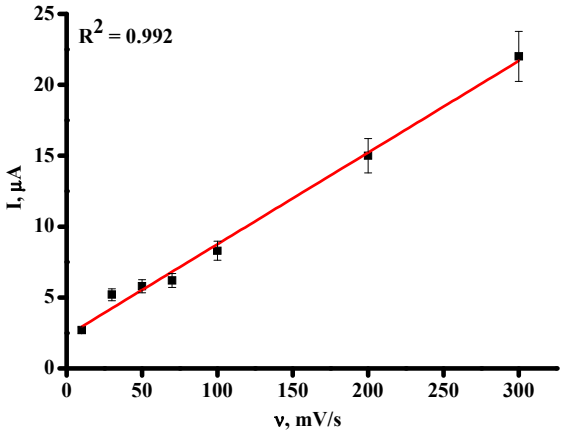

(**B**)

Figure 2. *Cont.*

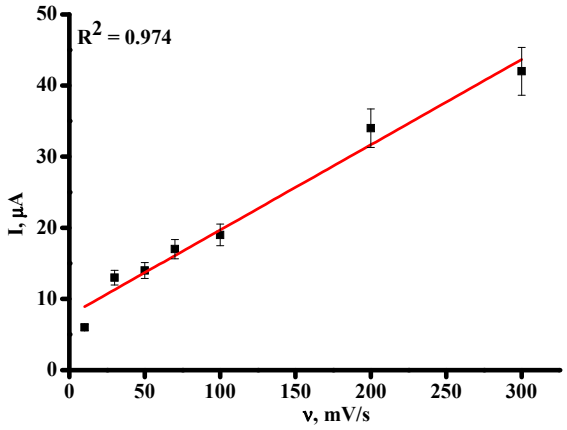

(**C**)

Figure 2. (**A**) CV of dsDNA (1.5 mg/mL) on SPE/SWCNT in the range of potentials of 0 V to 1.2 V at scan rates from 10 to 300 mV/s. Dependence between guanine (**B**) and adenine (**C**) peak currents and the scan rate.

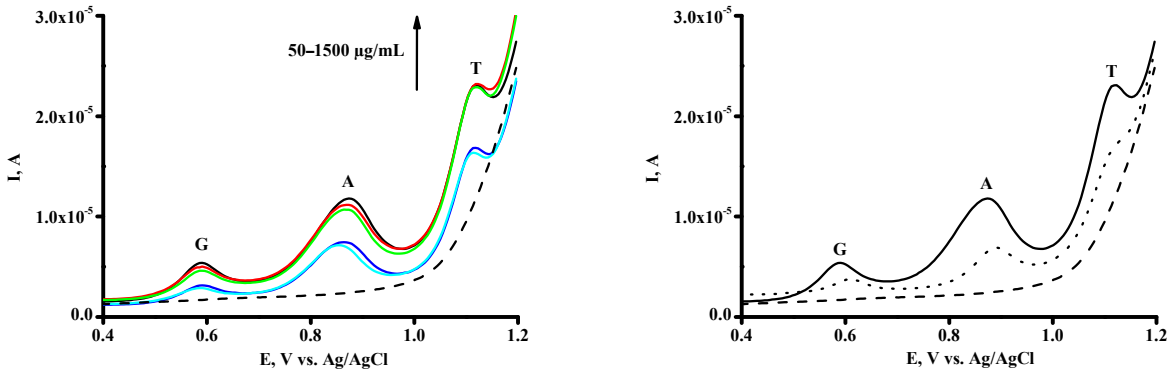

(**A**) (**B**)

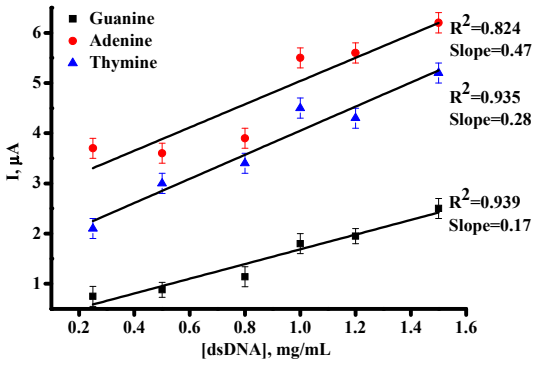

(**C**)

Figure 3. (**A**) DP voltammograms for SPE/SWCNT after deposition of dsDNA in the concentration range of 50–1500 µg/mL, SPE/SWCNT (dash line); (**B**) DP voltammograms for SPE/SWCNT (dash line) after deposition of DNA 1500 µg/mL (-) first scan, (. . .) second scan; (**C**) Calibration graph presenting the oxidative peak current I_G of guanine (G) residues at E = 0.59 ± 0.01 V, I_A of adenine (A) residues at E = 0.88 ± 0.01 V, I_T thymine (T) residues at E = 1.12 ± 0.01 V versus the concentration of dsDNA.

As can be seen from Figure 3A, modification of SPE with SWCNT dispersion in carboxymethylcellulose permits to analyse dsDNA with good sensitivity and broad concentration range of 50–1500 μg/mL. Analytical characteristics of SPE/SWCNT with dsDNA are presented in Table 2. It is important to underline that using DPV we can register simultaneously purine bases guanine, adenine, and pyrimidine base thymine (Figure 3A). The comparison of the first and the second scan of DPV of DNA confirmed the irreversible mode of nucleobases electrochemical oxidation (Figure 3B) [26–28,36,38]. The method of DNA registration represents a suitable platform for the researching of drug/DNA interaction for pharmacogenomic studies.

Table 2. Electroanalytical parameters of dsDNA on SPE/SWCNT using DPV technique.

Parameters	Guanine (G)	Adenine (A)	Thymine (T)
E_{ox}, V	0.59 ± 0.01	0.88 ± 0.01	1.12 ± 0.05
Sensitivity, μA/(μg × mL^{-1})	0.17	0.47	0.28
Linear range, μg/mL	50–1500	50–1500	50–1500
Equation for linear regression *	I_G = 1.47 ± 0.17 [dsDNA] + 0.22 ± 0.16	I_A = 2.31 ± 0.47 [dsDNA] + 2.72 ± 0.45	I_T = 2.40 ± 0.28 [dsDNA] + 1.65 ± 0.27
Correlation coefficient, R^2	0.939	0.824	0.935

* *I* corresponds to the oxidative currents (peak heights) for dsDNA; [dsDNA] is a concentration of dsDNA in μg/mL that was deposited onto the working surface area of SPE/SWCNT.

It is important to note that dilution of DNA with electrolyte buffer (PBS, pH 7.4) decreases in peak current intensity of heterocyclic nucleobases, however the values of potentials of electrochemical oxidation of G, A, and T were not shifted. The prepared SPE/SWCNT may act as sensing surface for the investigation of DNA-Umi interaction.

3.3. Investigation of the Interaction between Umi or NUmi and dsDNA

Understanding the mechanism of drug-DNA interactions is one of key topics in pharmacogenomics and drug toxicity assay. We used quantitative electrochemical analysis of dsDNA based on direct electrochemical oxidation of guanine, adenine, and thymine residues, and applied this technique for the comparative investigation of the interactions of Umi with DNA. The investigations were carried out using the increased concentration of umifenovir and measuring the differential pulse voltammetry peak current intensity of G, A, and T oxidation of constant concentration of dsDNA (1.5 mg/mL) immobilized on single-use SPE/SWCNT. Peaks of G, A, and T heterocyclic bases permits to register three active participants of binding events (Figure 4A).

It may be assumed that Umi–DNA interaction is accompanied with a decrease in the ability of G, A, and T moieties to be oxidized. No changes in G, A, and T peak height were observed when dsDNA sensor was incubated in blank phosphate buffer pH 7.4, for 30 min without the addition of drug. Umi has relatively low toxicity for humans (LD50 > 4 g kg^{-1}) and daily dosages of preventative and therapeutic dosages were defined as 200 mg and 800 mg/day, respectively, with a duration of medication of 5 days [8]. Based on these concentrations we used drug range of 10–150 μM for the investigation of the interaction of DNA with Umi (Figure 4A,B).

The interaction of Umi and NUmi with dsDNA studied at physiological pH 7.4 in PBS is accompanied by a decrease of DPV oxidation signals of heterocyclic bases. As can be seen from Figure 4A, an addition of different concentrations of Umi within a concentration range from 10 to 150 μM to the dsDNA, results in a clear and pronounced decrease of DPV oxidation signals of guanine, adenine, and thymine. The signal loss depended on the increasing concentration of Umi (Figure 4B). Additionally, we have registered the readable negative shift of oxidation potential of heterocyclic nucleobases corresponding to 40–60 mV for guanine, adenine, and thymine with increasing Umi concentration. The negative shift of oxidation potential reflects the binding mode of DNA-drug via electrostatic attraction assisted groove-binding interactions [26–28,36,38,39]. The same tendencies were registered for NUmi (Figure 4C). Umi molecule contains two tertiary nitrogen atoms which can be protonated resulting in salt or electrostatic bonds formation. Based on the values of oxidation current of nucleobases during interaction of drug with dsDNA the binding

constants for the complex were calculated using the following Equations (2)–(3) with constant DNA concentration [26–28,36,39–47].

$$[\text{DNA}] + [\text{drug}] \leftrightarrow [\text{DNA} \times \text{drug}], \quad (2)$$

$$K_b = [\text{DNA} \times \text{drug}]/([\text{DNA}] \times [\text{drug}]), \quad (3)$$

$$K_b \approx (I_{DNA} - I)/(I_{DNA} \times ([\text{drug}] - (I_{DNA} - I)), \quad (4)$$

where K_b corresponds to the binding constant, I_{DNA} corresponded to the peak current of dsDNA, I referred to the peak current for complex [dsDNA × Umi] at different Umi concentration.

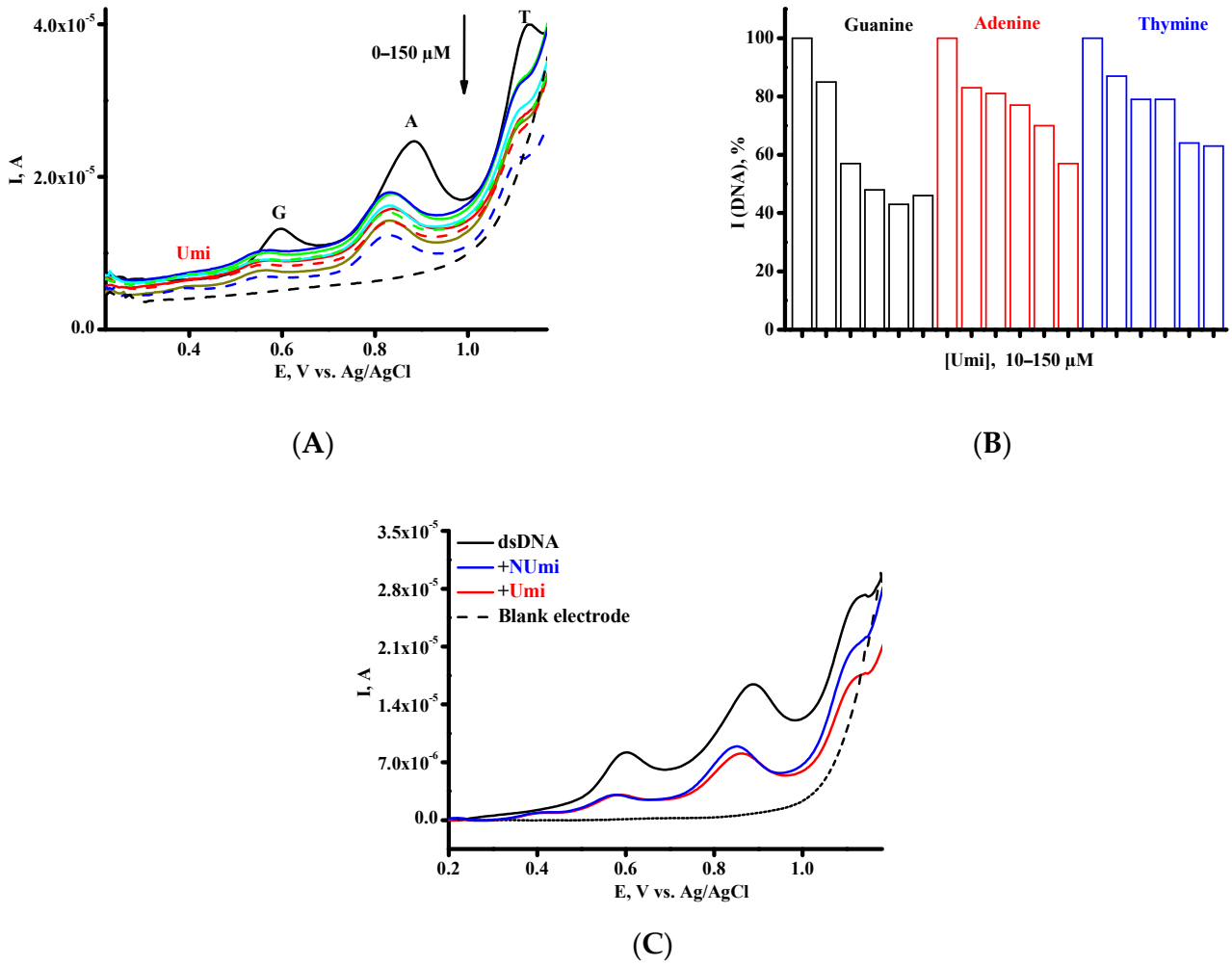

Figure 4. (**A**) DP voltammograms of dsDNA in the absence (black line) and in the presence of Umi in the concentration range of 10–150 µM, SPE/SWCNT (dash line); (**B**) Histograms corresponding to the average guanine, adenine, and thymine signals after the addition of Umi in the range of concentration 10–150 µM; (**C**) DP voltammograms of dsDNA in the absence (black line) and in the presence of 70 µM Umi (red line) and in the presence of 70 µM NUmi (blue line), SPE/SWCNT (dash line).

The concentration of dsDNA corresponded to peak height calculated either for A, G, and T peaks. The concentrations of complexed drug [DNA × drug] assumed to be proportional to the ($I_{DNA} - I$), where I_{DNA} and I are the peak currents of dsDNA in the absence and in the presence of Umi, respectively. Therefore, the Equation (3) can be transformed to Equation (4) [39–47].

Intercalation-based interactions are characterized with high K_b values usually 10^4–10^6 M^{-1}, while the lower K_b values implies a rather weaker interaction such as groove

or electrostatic interactions [22–25]. As can be seen from Table 3, the values of K_b reflect electrostatic and groove binding of drugs with dsDNA molecule. The negative shift of oxidation potential also verifies the DNA-drug interaction via electrostatic attraction assisted groove binding [26–28,39–47]. However, some contribution of hydrophobic interactions cannot be excluded based on the structure of Umi.

Table 3. Values of binding constants (K_b) of Umi or NUmi with dsDNA complex calculated from the results of DPV analysis.

Drug-DNA Complex	K_b, M^{-1}		
	G Peak	A Peak	T Peak
[Umi × DNA]	2.8×10^4	5.7×10^4	4.7×10^4
[NUmi × DNA]	1.1×10^5	4.4×10^4	8.2×10^3

The changes in the Gibbs free energy (ΔG) were calculated using the Equation (5):

$$\Delta G = -RT\ln K_b, \quad (5)$$

where K_b corresponds to the binding constant, R is gas constant, 8.3145 J $K^{-1}mol^{-1}$, T is temperature, in Kelvin.

The negative ΔG values (Table 4) were obtained in the range of −25.30 to −27.05 kJ mol^{-1}, confirming the spontaneous process for complex formation and more strong interaction with adenine base.

Table 4. Values of the Gibbs free energy (ΔG) for Umi or NUmi with dsDNA complex calculated for G, A, and T heterocyclic bases.

Drug-DNA Complex	ΔG, kJ/mol		
	G	A	T
[Umi × DNA]	−25.30	−27.05	−26.58
[NUmi × DNA]	−28.68	−26.41	−22.26

Based on the calculated values of K_b and shifts of peak potential we assume that Umi bind to dsDNA with formation of single complex via electrostatic interaction assisted groove binding [39–47].

DNA-mediated the electrochemical decline coefficient at each Umi or NUmi concentration can be estimated as a value of the percentage of nucleobases peak height decrees (S, %) using Equation (6) in accordance with [20,48,49]:

$$S = (S_s/S_b) \times 100\%, \quad (6)$$

where S_b and S_s are nucleobase oxidation signals before and after interaction of the Umi or NUmi with dsDNA, respectively. According to accepted criteria, a drug does not have a significant effect on DNA if S is higher than 85%; a moderate effect if the S parameter is between 50 and 85%, and a drug has a high effect on DNA if S is below 50% [20,40,48,49].

Based on our results we can assume that Umi and NUmi had non-toxic effect and moderate toxic effect in the range of concentrations 10–100 μM (Figure 5A–C). These drug concentrations are therapeutically relevant, so the influence of antiviral drug umifenovir on DNA (DNA-mediated toxicity based on guanine electrochemical signals) appears only at higher concentration in the window of 100–150 μM [50].

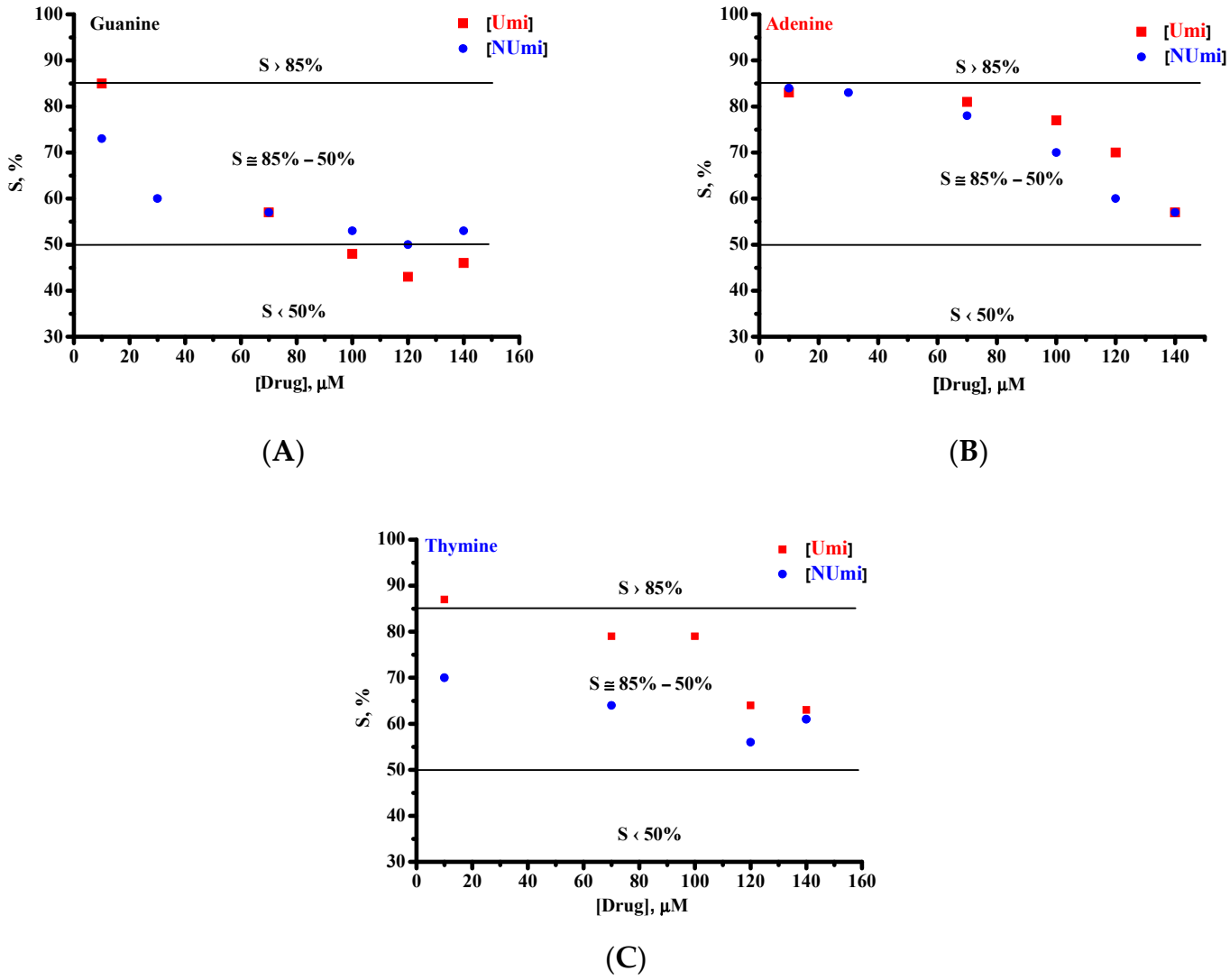

Figure 5. The influence of antiviral drug umifenovir (Umi) and umifenovir encapsulated in phospholipids micelles (nanosome/umifenovir, NUmi) in the concentration range of 10–150 μM on DNA oxidation signals of (**A**) guanine, (**B**) adenine and (**C**) thymine. *S*, %—DNA-mediated the electrochemical decline coefficient.

4. Conclusions

DNA is not only the target for medications, but also has potential as a promising drug-loadable polymeric platform [17,51,52]. From this viewpoints investigation of drug-DNA interactions is a key for the pharmacogenomic studies and construction of new drug-delivery systems. In this paper, electrochemical behavior of antiviral drug umifenovir and umifenovir encapsulated in phospholipids micelles was investigated for the first time. We have shown that Umi can be electro oxidized at the potential of +0.388 ± 0.002 V. Non-overlapping signatures of dsDNA and umifenovir permit to register with high sensitivity complex formation of drug with purine and pyrimidine heterocyclic bases separately. Many active pharmaceutical ingredients contain a nitrogen atom that can be protonated at physiologically relevant media, resulting in salt formation, which in turn, lead to electrostatic interaction with targeted DNA molecule. The values of binding constants for drug-DNA complex formation also confirmed the electrostatic mode of integration. The negative values of the change in the Gibbs free energy prove the spontaneous character of binding processes. The cathodic shifts of oxidation potentials for heterocyclic bases serve as further evidence of electrostatic interaction between umifenovir and umifenovir

encapsulated in phospholipids micelles and DNA, corresponding to 40–60 mV for guanine, adenine, and thymine with increasing drug concentration. Electrochemical biosensing of drug—DNA nano complexes formation is promising technology for pharmacogenomics, for the assessment of interactions new chemicals (as potential antivirus drug) with virus RNA and DNA molecules. Electroanalysis of DNA/RNA molecules is multiparametric method, which permits to calculate quantitation characteristics of specific binding events.

As have been shown earlier, one of the ways to increase the bioavailability, therapeutic efficacy of drugs, reduce their toxicity, and decline side effects is to use phospholipids nanoparticle as drug delivery systems [13,14,53]. Based on the properties of nanosome rifampicin, doxorubicin, chlorine E6, prednisolone [13,14], it is possible to assume that NUmi will have improves pharmacological characteristics as antivirus drug in comparison with Umi.

Author Contributions: V.V.S. developed the concept and methodology; T.V.B. performed electrochemical experiments and analyzed the obtained data; L.E.A. prepared an original draft, carried out a review and editing; V.V.P. calculated the binding constants and changes in the Gibbs free energy for drug-DNA complex; L.V.K. provided the antiviral drug umifenovir for investigation, carried out a review and editing. All authors have read and agreed to the published version of the manuscript.

Funding: The study was performed using "Avogadro" large-scale research facilities and was financially supported by the Ministry of Education and Science of the Russian Federation, Agreement No. 075-15-2021-933, unique project ID: RF00121X0004.

Data Availability Statement: Not applicable.

Conflicts of Interest: The authors declare no conflict of interest.

References

1. Jena, N. Drug targets, mechanisms of drug action, and therapeutics against SARS-CoV-2. *Chem. Phys. Impact* **2021**, *2*, 100011. [CrossRef]
2. Wang, X.; Cao, R.; Zhang, H.; Liu, J.; Xu, M.; Hu, H.; Li, Y.; Zhao, L.; Li, W.; Sun, X.; et al. The anti-influenza virus drug, arbidol is an efficient inhibitor of SARS-CoV-2 in vitro. *Cell Disc.* **2020**, *6*, 28. [CrossRef] [PubMed]
3. Pécheur, E.-I.; Borisevich, V.; Halfmann, P.; Morrey, J.; Smee, D.; Prichard, M.; Mire, C.; Kawaoka, Y.; Geisbert, T.; Polyak, S. The synthetic antiviral drug arbidol inhibits globally prevalent pathogenic viruses. *J. Virol.* **2016**, *90*, 3086–3092. [CrossRef] [PubMed]
4. Proskurnina, E.; Izmailov, D.; Sozarukova, M.; Zhuravleva, T.; Leneva, I.; Poromov, A. Antioxidant potential of antiviral drug umifenovir. *Molecules* **2020**, *25*, 1577. [CrossRef]
5. Deng, P.; Zhong, D.; Yu, K.; Zhang, Y.; Wang, T.; Chen, X. Pharmacokinetics, Metabolism, and Excretion of the Antiviral Drug Arbidol in Humans. *Antimicrob. Agents Chemother.* **2013**, *57*, 1743–1755. [CrossRef]
6. Tarighi, P.; Eftekhari, S.; Chizari, M.; Sabernavaei, M.; Jafari, D.; Mirzabeigi, P. A review of potential suggested drugs for coronavirus disease (COVID-19) treatment. *Eur. J. Pharmacol.* **2021**, *895*, 173890. [CrossRef]
7. Kumar, D.; Trived, N. Disease-drug and drug-drug interaction in COVID-19: Risk and assessment. *Biomed. Pharmacother.* **2021**, *139*, 111642. [CrossRef]
8. Yang, C.; Ke, C.; Yue, D.; Li, W.; Hu, Z.; Liu, W.; Hu, S.; Wang, S.; Liu, J. Effectiveness of arbidol for COVID-19 prevention in health professionals. *Front. Public Health* **2020**, *8*, 249. [CrossRef]
9. Hanai, T. Quantitative in silico analysis of SARS-CoV-2 S-RBD omicron mutant transmissibility. *Talanta* **2022**, *240*, 123206. [CrossRef]
10. Crommelin, D.; van Hoogevest, P.; Storm, G. The role of liposomes in clinical nanomedicine development. What now? Now what? *J. Control. Release* **2020**, *318*, 256–263. [CrossRef]
11. Alavi, M.; Karimi, N.; Safaei, M. Application of Various Types of Liposomes in Drug Delivery Systems. *Adv. Pharm. Bull.* **2017**, *7*, 3–9. [CrossRef]
12. Sharma, D.; Ali, A.; Trivedi, L. An Updated Review on: Liposomes as drug delivery system. *PharmaTutor* **2018**, *6*, 50–62. [CrossRef]
13. Ipatova, O.; Torkhovskaya, T.; Medvedeva, N.; Prozorovsky, V.; Ivanova, N.; Shironin, A. Bioavailability of oral drugs and the methods for its improvement. *Biochem. Moscow Suppl. Ser. B* **2010**, *4*, 82–94. [CrossRef]
14. Tereshkina, Y.; Torkhovskaya, T.; Tikhonova, E.; Kostryukova, L.; Sanzhakov, M.; Korotkevich, E.; Khudoklinova, Y.; Orlova, N.; Kolesanova, E. Nanoliposomes as drug delivery systems: Safety concerns. *J. Drug Target.* **2022**, *30*, 313–325. [CrossRef]
15. Shumyantseva, V.; Kuzikov, A.; Masamrekh, R.; Bulko, T.; Archakov, A. From electrochemistry to enzyme kinetics of cytochrome P450. *Biosens. Bioelectron.* **2018**, *121*, 192–204. [CrossRef]
16. Kurbanoglu, S.; Dogan-Topal, B.; Rodriguez, E.; Bozal-Palabiyik, B.; Ozkan, S.; Uslu, B. Advances in electrochemical DNA biosensors and their interaction mechanism with pharmaceuticals. *J. Electroanal. Chem.* **2016**, *775*, 8–26. [CrossRef]

17. Hasanzadeh, M.; Shadjou, N. Pharmacogenomic study using bio- and nanobioelectrochemistry: Drug–DNA interaction. *Mater. Sci. Eng. C Mater. Biol. Appl.* **2016**, *61*, 1002–1017. [CrossRef]
18. Nikitin, M. Non-complementary strand commutation as a fundamental alternative for information processing by DNA and gene regulation. *Nat. Chem.* **2023**, *15*, 70–82. [CrossRef]
19. Sigolaeva, L.; Bulko, T.; Kozin, M.; Zhang, W.; Köhler, M.; Romanenko, I.; Yuan, J.; Schacher, F.; Pergushov, D.; Shumyantseva, V. Long-term stable poly(ionic liquid)/MWCNTs inks enable enhanced surface modification for electrooxidative detection and quantification of dsDNA. *Polymer* **2019**, *168*, 95–103. [CrossRef]
20. Krejcova- Sirlova, Z.; Barek, J.; Vyskocil, V. Voltammetric studies of the interaction of genotoxic 2-nitrofluorene with DNA. *Bioelectrochemistry* **2023**, *149*, 108326. [CrossRef]
21. Shumyantseva, V.; Bulko, T.; Tikhonova, E.; Sanzhakov, M.; Kuzikov, A.; Masamrekh, R.; Pergushov, D.; Schacher, F.; Sigolaeva, L. Electrochemical studies of the interaction of rifampicin and nanosome/rifampicin with dsDNA. *Bioelectrochemistry* **2021**, *140*, 107736. [CrossRef] [PubMed]
22. Morawska, K.; Popławski, T.; Ciesielski, W.; Smarzewska, S. Electrochemical and spectroscopic studies of the interaction of antiviral drug Tenofovir with single and double stranded DNA. *Bioelectrochemistry* **2018**, *123*, 227–232. [CrossRef] [PubMed]
23. Bolat, G. Investigation of poly(CTAB-MWCNTs) composite based electrochemical DNA biosensor and interaction study with anticancer drug Irinotecan. *Microchem. J.* **2020**, *159*, 105426. [CrossRef]
24. Graves, D.; Velea, L. Intercalative Binding of Small Molecules to Nucleic Acids. *Curr. Org. Chem.* **2005**, *4*, 915–929. [CrossRef]
25. Hatamluyi, B.; Es'haghi, Z. Quantitative Biodetection of Anticancer Drug Rituxan with DNA Biosensor Modified PAMAM Dendrimer/Reduced Graphene Oxide Nanocomposite. *Electroanalysis* **2018**, *30*, 1659–1668. [CrossRef]
26. Rupar, J.; Aleksić, M.; Dobričić, V.; Brborić, J.; Čudina, O. An electrochemical study of 9-chloroacridine redox behavior and its interaction with double-stranded DNA. *Bioelectrochemistry* **2020**, *135*, 107579. [CrossRef]
27. Vyskočil, V.; Blašková, M.; Hájková, A.; Horáková, E.; Krejčová, Z.; Stávková, K.; Wang, J. Electrochemical DNA biosensors—Useful diagnostic tools for the detection of damage to DNA caused by organic xenobiotics (A Review). *Sens. Electroanal.* **2012**, *7*, 141–162.
28. Ramotowska, S.; Ciesielska, A.; Makowski, M. What can electrochemical methods offer in determining DNA–drug interactions? *Molecules* **2021**, *26*, 3478. [CrossRef]
29. Held, P. Nucleic Acid Purity Assessment Using A260/A280 Ratios. In *Application Note*; BioTek Instruments Incorporation: Winooski, VT, USA, 2001; pp. 1–5.
30. Smith, P.; Jin, P.; Rahman, K. Strategies for drug repurposing against coronavirus targets. *Curr. Res. Pharmacol. Drug Discov.* **2022**, *3*, 100072. [CrossRef]
31. Carrara, S.; Baj-Rossi, C.; Boero, C.; De Micheli, G. Do Carbon Nanotubes contribute to Electrochemical Biosensing? *Electrochim. Acta* **2014**, *128*, 102–112. [CrossRef]
32. Nouri-Nigje, E.; Bischoff, R.; Bruins, A.; Permentier, H. Electrochemistry in the mimicry of oxidative drug metabolism by cytochrome P450s. *Curr. Drug Metab.* **2011**, *12*, 359–371. [CrossRef]
33. Jurva, U.; Wikström, H.; Weidolf, L.; Bruins, A. Comparison between electrochemistry/mass spectrometry and cytochrome P450 catalyzed oxidation reactions. *Rapid Commun. Mass Spectrom.* **2003**, *17*, 800–810. [CrossRef]
34. Gosser, D. *Cyclic Voltammtry*; VCH: New York, NY, USA, 1994.
35. Compton, B.; Banks, C. *Understanding Voltammetry*, 2nd ed.; Imperial College Press: London, UK, 2011.
36. Brett, C.M.A.; Oliveira Brett, A.M. *Electrochemistry: Principles, Methods, and Applications*, 1st ed.; Oxford Science University Publications: Oxford, UK, 1993; p. 219. [CrossRef]
37. Miller, J.; Miller, J.C. *Statistics and Chemometrics for Analytical Chemistry*, 7th ed.; Pearson: London, UK, 2018; Available online: https://www.pearson.com/uk/educators/higher-education-educators/program/Miller-Statistics-and-Chemometrics-forAnalytical-Chemistry-7th-Edition/PGM2061238.html (accessed on 10 May 2020).
38. Ferapontova, E. DNA electrochemistry and electrochemical sensor for nucleic acids. *Ann. Rev. Anal. Chem.* **2018**, *11*, 197–218. [CrossRef]
39. Findik, M.; Bingol, H.; Erdem, A. Hybrid nanoflowers modified pencil graphite electrodes developed for electrochemical monitoring of interaction between Mitomycin C and DNA. *Talanta* **2021**, *222*, 121647. [CrossRef]
40. Bagni, G.; Osella, D.; Sturchio, E.; Macsini, M. Deoxyribonucleic acid (DNA) biosensors for environmental risk assessment and drug studies. *Anal. Chim. Acta* **2006**, *573*, 81–89. [CrossRef]
41. Chiorcea-Paquim, A.-M.; Oliveira-Brett, A.-M. DNA Electrochemical Biosensors for In Situ Probing of Pharmaceutical Drug Oxidative DNA Damage. *Sensors* **2021**, *21*, 1125. [CrossRef]
42. Erdem, A.; Muti, M.; Papakonstantinou, P.; Canavar, E.; Karadeniz, H.; Congur, G.; Sharma, S. Graphene oxide integrated sensor for electrochemical monitoring of mitomycin C–DNA interaction. *Analyst* **2012**, *137*, 2129–2135. [CrossRef]
43. Eksin, E.; Zor, E.; Erdem, A.; Bingöl, H. Electrochemical monitoring of biointeraction by graphene-based material modified pencil graphite electrode. *Biosens. Bioelectron.* **2017**, *92*, 207–214. [CrossRef]
44. Fotouhi, L.; Bahmani, F. MWCNT Modified Glassy Carbon Electrode: Probing Furazolidone-DNA Interactions and DNA Determination. *Electroanalysis* **2013**, *25*, 757–764. [CrossRef]
45. Sirajuddin, M.; Ali, S.; Badshah, A. Drug–DNA interactions and their study by UV–vis, fluorescence spectroscopies and cyclic voltammetry. *J. Photochem. Photobiol. B Biol.* **2013**, *124*, 1–19. [CrossRef]

46. Dogan-Topal, B.; Bozal-Palabiyik, B.; Ozkan, S.; Uslu, B. Investigation of anticancer drug lapatinib and its interaction with dsDNA by electrochemical and spectroscopic techniques. *Sens. Actuators B Chem.* **2014**, *194*, 185–194. [CrossRef]
47. Temerk, Y.; Ibrahim, M.; Ibrahim, H.; Kotb, M. Interactions of an anticancer drug lomustine with single and double stranded DNA at physiological conditions analysed by electrochemical and spectroscopic methods. *J. Electroanal. Chem.* **2016**, *769*, 62–71. [CrossRef]
48. Muti, M.; Muti, M. Electrochemical monitoring of the interaction between anticancer drug and DNA in the presence of antioxidant. *Talanta* **2018**, *178*, 1033–1039. [CrossRef] [PubMed]
49. Agafonova, L.; Tikhonova, E.; Sanzhakov, M.; Kostryukova, L.; Shumyantseva, V. Electrochemical Studies of the Interaction of Phospholipid Nanoparticles with dsDNA. *Processes* **2022**, *10*, 2324. [CrossRef]
50. Carrara, S.; Cavallini, A.; Erokhin, V.; De Micheli, G. Multi-panel drugs detection in human serum for personalized therapy. *Biosens. Bioelectron.* **2011**, *26*, 3914–3919. [CrossRef]
51. Mohammad, S.; Choi, Y.; Chung, J.; Cedrone, E.; Neun, B.; Dobrovolskaia, M.; Yang, X.; Guo, W.; Chew, Y.; Kim, J.; et al. Nanocomplexes of doxorubicin and DNA fragments for efficient and safe cancer chemotherapy. *J. Control. Release* **2023**, *354*, 91–108. [CrossRef]
52. Evtugyn, G.; Porfireva, A.; Belyakova, S. Electrochemical DNA sensors for drug determination. *J. Pharmac. Biomed. Anal.* **2022**, *221*, 115058. [CrossRef]
53. Hashemi, M.; Ghadyani, F.; Hasani, S.; Olyaee, Y.; Raei, B.; Khodadadi, M.; Ziyarani, M.; Basti, F.; Tavakolpournegari, A.; Matinahmadi, A.; et al. Nanoliposomes for doxorubicin delivery: Reversing drug resistance, stimuli-responsive carriers and clinical translation. *J. Drug Deliv. Sci. Technol.* **2023**, *80*, 104112. [CrossRef]